

Dalton Transactions

Accepted Manuscript



This is an *Accepted Manuscript*, which has been through the Royal Society of Chemistry peer review process and has been accepted for publication.

Accepted Manuscripts are published online shortly after acceptance, before technical editing, formatting and proof reading. Using this free service, authors can make their results available to the community, in citable form, before we publish the edited article. We will replace this *Accepted Manuscript* with the edited and formatted *Advance Article* as soon as it is available.

You can find more information about *Accepted Manuscripts* in the [Information for Authors](#).

Please note that technical editing may introduce minor changes to the text and/or graphics, which may alter content. The journal's standard [Terms & Conditions](#) and the [Ethical guidelines](#) still apply. In no event shall the Royal Society of Chemistry be held responsible for any errors or omissions in this *Accepted Manuscript* or any consequences arising from the use of any information it contains.



Journal Name

ARTICLE

Porous Frameworks Constructed by Non-Covalent Linking of Substitution-Inert Metal Complexes

Received 00th January 20xx,
Accepted 00th January 20xx

DOI: 10.1039/x0xx00000x

www.rsc.org/

Takahiro Itoh,^{a,b} Mio Kondo,^{*a,b,c,d} Hirotoshi Sakamoto,^e Kaori Wakabayashi,^a Mari Kanaike,^a Kenichiro Itami,^{e,f,g} and Shigeyuki Masaoka^{*a,b,d}

The incorporation of active sites into metal-organic frameworks (MOFs) or porous coordination polymers (PCPs) is an attractive way to functionalize these materials. However, the methodology to organize substitution-inert metal-based secondary building units (SBUs) with active sites into MOFs or PCPs *via* coordination driven self-assembly is severely limited. In this study, we successfully assembled substitution-inert paddle-wheel Rh(II) dimers to afford three novel porous frameworks, Rh₂(ppeb)₄(THF)₂ (**1-THF**), Rh₂(ppeb)₄(3-pentanone)₂ (**1-PN**) and Rh₂(ppeb)₄(1-adamantylamine)₂ (**1-AD**) (ppeb = 4-[(perfluorophenyl)ethynyl]benzoate), by using non-covalent interactions. Multipoint arene-perfluoroarene (Ar-Ar^f) interactions, which allow in the unidirectional face-to-face interaction mode of aromating rings, were used to assemble substitution-inert paddle-wheel Rh(II) dimers. The obtained frameworks were structurally characterized by single crystal X-ray diffraction, and it is found that all structures exhibited a one-dimensional channel with active axial sites exposed to the pores. The porous properties of the obtained frameworks were also investigated by thermogravimetric analysis, gas adsorption and powder X-ray diffraction measurements. Moreover, the ligand substitution reaction at the active axial sites was examined at the crystalline state and the flexible structural transformation with the change of channel shapes and sizes was observed.

Introduction

Metal-organic frameworks (MOFs) or porous coordination polymers (PCPs)^{1,2} are crystalline materials composed of inorganic building units and organic linkers and have attracted

considerable attention as new types of porous materials. In particular, MOFs or PCPs with open metal sites are of interest because these sites can strongly interact with adsorbed molecules to afford specific functionalisation of the pore surfaces for adsorption/separation,³ heterogeneous catalysis,⁴ and sensing.⁵ One of the most straightforward strategies to

^a Mr. T. Itoh, Dr. M. Kondo, Ms. K. Wakabayashi, Ms. M. Kanaike, and Prof. Dr. S. Masaoka

Department of Life and Coordination-Complex Molecular Science
Institute for Molecular Science
5-1 Higashiyama, Myodaiji, Okazaki, Aichi 444-8787, Japan.
E-mail: mio@ims.ac.jp, masaoka@ims.ac.jp

^b Mr. T. Itoh, Dr. M. Kondo, and Prof. Dr. S. Masaoka
SOKENDAI [The Graduate University for Advanced Studies]
Shonan Village, Hayama, Kanagawa 240-0193, Japan.

^c Dr. M. Kondo
ACT-C, Japan Science and Technology Agency (JST)
4-1-8 Honcho, Kawaguchi, Saitama 332-0012, Japan.

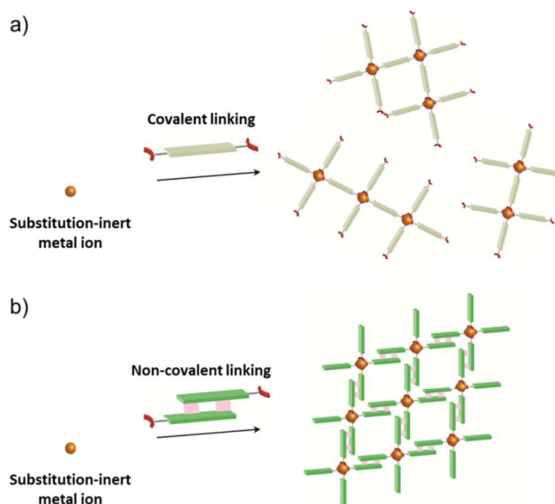
^d Dr. M. Kondo, and Prof. Dr. S. Masaoka
Research Center of Integrative Molecular Systems (CIMoS)
Institute for Molecular Science
38 Nishigo-naka, Myodaiji, Okazaki, Aichi 444-8585, Japan.

^e Dr. H. Sakamoto and Prof. Dr. K. Itami
JST, ERATO, Itami Molecular Nanocarbon Project
Chikusa, Nagoya 464-8602, Japan

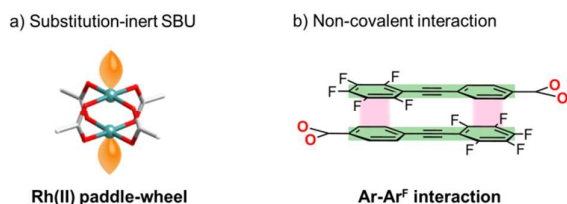
^f Prof. Dr. K. Itami
Graduate School of Science, Nagoya University,
Chikusa, Nagoya 464-8602, Japan

^g Prof. Dr. K. Itami
Institute of Transformative Bio-Molecules (WPI-ITbM),
Nagoya University, Nagoya 464-8602, Japan

Electronic Supplementary Information (ESI) available: Figures of CO₂ or N₂ sorption isotherms, PXRD patterns. CCDC 1049445–1049447. For ESI and crystallographic data in CIF or other electronic format see DOI: 10.1039/x0xx00000x



Scheme 1 Schematic illustration of the self-assembly of substitution-inert SBUs via (a) covalent linking and (b) non-covalent linking.



Scheme 2 Schematic illustration of (a) substitution inert SBU and (b) non-covalent interaction employed in this study.

construct such materials is to embed open metal sites on secondary building units (SBUs) of the framework.⁶ The Rh(II) paddle-wheel complex, which is composed of four substitution-inert carboxylate ligands and two substitution-labile axial ligands, would be an attractive SBU with D_{4h} symmetry because the porous frameworks constructed are expected to show high stability arising from the substitution-inert carboxylate ligands and the high reactivity of the substitution-labile axial sites known as active centres for many catalytic reactions.⁷ However, it is hard to construct MOFs or PCPs by linking substitution-inert metal-based SBUs *via* covalent linkers (Scheme 1a) because the covalent linking of these SBUs often prevents the formation of single crystalline materials.⁸ Although there are many reports on single crystal structures of MOFs and PCPs consisting of substitution-labile SBUs with active sites (e.g., HKUST-1,^{6a} MOF-74,^{6b} and so on⁹), to the best of our knowledge, no single crystal structures of MOFs or PCPs constructed by substitution-inert SBUs with those sites have been reported so far.

Here, we show an effective approach to construct a porous framework based on substitution-inert SBUs with active sites. Recently, many reports have proved that non-covalent interactions (e.g., hydrogen bonds,¹⁰ π - π interactions,¹¹ combination of hydrogen bonds and π - π interactions,¹² and van der Waals interactions¹³) can be promising tools for construction of porous materials. In comparison to covalent linking, these interactions can work in ambient condition to afford comparable well-defined framework. A key to our success is the usage of this “non-covalent” interaction (Scheme 1b) for the self-assembly of Rh(II) paddle-wheel dimers (Scheme 2a). As a module for non-covalent linking, a monocarboxylate ligand with multipoint arene-perfluoroarene¹⁴ (Ar-Ar^F) interaction sites was designed (Scheme 2b). As we previously reported that this interaction enabled the unidirectional face-to-face interaction mode of aromatic rings to work dominantly, and the controlled self-assembly of molecules can be achieved.¹⁵

Experimental

General Methods

All solvents and reagents are of the highest quality available and used as received except for diethylamine and triethylamine. Diethylamine and triethylamine were dried by reflux over KOH, distilled under argon, and degassed with a freeze-and-pump thaw. 4-[[perfluorophenyl]ethynyl]benzoic

acid (Hppeb) and $\text{Na}_4[\text{Rh}_2(\text{CO}_3)_4]$ were prepared by the literature methods.^{15,16} All syntheses were performed under an atmosphere of dry nitrogen or dry argon unless otherwise indicated. Elemental analysis was carried out on a J-SCIENCE LAB MICRO CORDER JM10 elemental analyser. ¹H NMR spectrum was acquired on a JEOL JNM-LA500 spectrometer, where chemical shifts in $\text{DMF-}d_7$ were referenced to internal tetramethylsilane. ¹⁹F NMR spectrum was acquired on a JEOL JNM-LA500 spectrometer, where chemical shifts in $\text{DMF-}d_7$ were referenced to external trifluorotoluene. Thermogravimetric analyses (TGA) were carried out with a SHIMADZU DTG-60 under a nitrogen atmosphere. TGA profiles of **1-THF**, **1-PN** and **1-AD** were measured with a heating rate of 20 K min⁻¹. Fourier transformed infrared spectra were measured on a Perkin-Elmer Spectrum 100 FT-IR spectrometer equipped with an ATR (Attenuated Total Reflectance) accessory.

Synthetic Procedures

Synthesis of $\text{Rh}_2(\text{ppeb})_4(\text{Et}_2\text{O})_2$. $\text{Na}_4[\text{Rh}_2(\text{CO}_3)_4] \cdot 3\text{H}_2\text{O}$ (59 mg, 0.10 mmol) and Hppeb (250 mg, 0.80 mmol) in 40 ml of DMA/ H_2O mixed solvents were stirred for 8 h at 100 °C. After evaporation of the solvent, the residue was washed with water and dissolved in Et_2O and subsequently purified by column chromatography using neutral alumina (Et_2O as eluent). The yield of $[\text{Rh}_2(\text{ppeb})_4]$ was 44 mg (27% based on $\text{Na}_4[\text{Rh}_2(\text{CO}_3)_4] \cdot 3\text{H}_2\text{O}$). ¹H NMR (500 MHz, $\text{DMF-}d_7$) δ ppm: 7.64 (d, $J = 10.0$ Hz, 2H), 7.98 (d, $J = 10.0$, 2H); ¹⁹F NMR (470.4 MHz, $\text{DMF-}d_7$) δ ppm: -164.3 (dt, $J = 4.7, 18.8$ Hz, 2F), -154.5 (t, $J = 18.8$ Hz, 1F), -138.9 (dd, $J = 4.7, 18.8$ Hz, 2F); Anal. Calcd. for $\text{Rh}_2(\text{O}_2\text{CC}_6\text{H}_4\text{C}_2\text{C}_6\text{F}_5)_4(\text{Et}_2\text{O})_2 \cdot 2\text{H}_2\text{O}$: C, 49.96; H, 2.60; N, 0.00%. Found: C, 49.79; H, 2.60; N, 0.13%.

Syntheses of **1-THF, **1-PN**, **1-AD**.** The three kinds of axial ligand substituted complexes were synthesised by the recrystallization of $\text{Rh}_2(\text{ppeb})_4(\text{Et}_2\text{O})_2$. $\text{Rh}_2(\text{ppeb})_4(\text{THF})_2$ (**1-THF**), $\text{Rh}_2(\text{ppeb})_4(3\text{-pentanone})_2$ (**1-PN**) were obtained by the slow evaporation of the mixed solution of $\text{Et}_2\text{O}/\text{THF}$ and $\text{Et}_2\text{O}/3\text{-pentanone}$ containing $\text{Rh}_2(\text{ppeb})_4(\text{Et}_2\text{O})_2$, respectively. For $\text{Rh}_2(\text{ppeb})_4(1\text{-adamantylamine})_2$ (**1-AD**), the recrystallisation was performed by layering the Et_2O solution of 1-adamantylamine on the Et_2O solution of $\text{Rh}_2(\text{ppeb})_4(\text{Et}_2\text{O})_2$. FTIR-ATR (cm^{-1}): 441w, 466s, 522s, 583w, 646m, 699m, 761s, 774s, 850m, 861m, 884m, 965s, 988s, 1018w, 1042w, 1113m, 1141w, 1176w, 1286w, 1389s, 1496s, 1523m, 1549w, 1597m (COO⁻), 2227w (C≡C), 2876w, 2978w (**1-THF**). FTIR-ATR (cm^{-1}): 411m, 465s, 522s, 582w, 645m, 699m, 725w, 761s, 774s, 813w, 859m, 964s, 989s, 1020m, 1113m, 1143w, 1178m, 1250w, 1288m, 1305m, 1391s, 1483m, 1496s, 1523m, 1548m, 1596m (COO⁻), 1677m, 1718w, 2227w (C≡C), 2980w (**1-PN**). FTIR-ATR (cm^{-1}): 403w, 428w, 463s, 520s, 644m, 698m, 717w, 762s, 773s, 849m, 860m, 924m, 965s, 988s, 1017m, 1061w, 1094w, 1115m, 1141w, 1178w, 1290w, 1311w, 1385s, 1450w, 1496s, 1523m, 1547w, 1600m (COO⁻), 2228w (C≡C), 3275w (NH₂), 3333w(NH₂) (**1-AD**).

X-ray Crystallography

Table 1 Crystallographic data and structural refinements for **1-THF**, **1-PN** and **1-AD**

Compound	1-THF	1-PN	1-AD
Formula	C ₆₈ H ₃₂ F ₂₀ O ₁₀ Rh ₂	C ₁₇₀ H ₁₃₂ F ₄₀ O ₂₆ Rh ₄	C ₉₂ H ₇₀ F ₂₀ N ₂ O ₁₁ Rh ₂
Formula weight	1594.76	3762.40	1965.32
Temperature (°C)	-150	-150	-150
Crystal system	Monoclinic	Triclinic	Triclinic
Space group	<i>C2/m</i> (#12)	<i>P</i> -1 (#2)	<i>P</i> -1 (#2)
<i>a</i> (Å)	18.6449(7)	15.1526(7)	10.8625(8)
<i>b</i> (Å)	27.2267(14)	15.3844(4)	13.8827(10)
<i>c</i> (Å)	8.8932(4)	19.5087(4)	14.9217(11)
α (deg)	90	99.0550(7)	103.6458(15)
β (deg)	107.4822(12)	96.0045(7)	93.1519(15)
γ (deg)	90	112.8590(4)	94.0312(16)
<i>V</i> (Å ³)	4306.0(3)	4069.14(17)	2175.3(3)
<i>Z</i>	2	1	1
<i>D</i> _c (g cm ⁻³)	1.230	1.535	1.500
μ (mm ⁻¹)	0.471	0.514	0.483
<i>F</i> (000)	1580	1900	994
<i>R</i> ₁ ^a	0.0660	0.0554	0.0511
<i>wR</i> ₂ ^b	0.1742	0.1875	0.1511
Goodness-of-fit on <i>F</i> ²	1.135	1.111	1.089

$$^a R_1 = \frac{\sum ||F_o| - |F_c||}{\sum |F_o|}, \quad ^b wR_2 = \frac{[\sum (w(F_o^2 - F_c^2)^2)]}{\sum w(F_o^2)^2}]^{1/2}.$$

Crystals of **1-THF**, **1-PN** and **1-AD** were mounted in a loop. Diffraction data at 123 K were measured on a RAXIS-RAPID Imaging Plate diffractometer equipped with confocal monochromated Mo-K α radiation and data was processed using RAPID-AUTO (Rigaku). Structures were solved by direct methods and refined by full-matrix least squares techniques on *F*² (SHELXL-97).¹⁷ All of the non-hydrogen atoms were anisotropically refined, while all of the hydrogen atoms (except for amine hydrogen atoms of 1-adamantylamine in **1-AD**, which were found on a difference Fourier map and refined isotropically) were placed geometrically and refined with a riding model with *U*_{iso} constrained to be 1.2 times the *U*_{eq} of the carrier atom. For **1-THF**, the diffused electron densities resulting from residual solvent molecules were removed from the data set using the SQUEEZE routine of PLATON and refined further using the data generated. CCDC reference numbers 1049445–1049447 (**1-THF**, **1-PN** and **1-AD**).

Crystal data for Rh₂(ppeb)₄(THF)₂ (1-THF**):** C₆₈H₃₂F₂₀O₁₀Rh₂, *M_r* = 1594.76, monoclinic, space group *C2/m*, (#12), *a* = 18.6449(7), *b* = 27.2267(14), *c* = 8.8932(4) Å, β = 107.4822(12)°, *V* = 4306.0(3) Å³, *Z* = 2, *T* = 123(2) K, ρ_c = 1.230 g cm⁻³, μ (Mo-K α) = 0.471 cm⁻¹, $2\theta_{\max}$ = 50.0°, λ (Mo-K α) = 0.71074 Å, 16842 reflections measured, 3892 unique (*R*_{int} = 0.0312), 3549 (*I* > 2 σ (*I*)) were used to refine 238 parameters, 6 restraints, *wR*₂ = 0.1742 (*I* > 2 σ (*I*)), *R*₁ = 0.0660 (*I* > 2 σ (*I*)), GOF = 1.135.

Crystal data for Rh₂(ppeb)₄(3-pentanone)₂ (1-PN**):** C₁₇₀H₁₃₂F₄₀O₂₆Rh₄, *M_r* = 3762.40, triclinic, space group *P*-1, (#2), *a* = 15.1526(7), *b* = 15.3844(4), *c* = 19.5087(4) Å, α = 99.0550(7)°, β = 96.0045(7)°, γ = 112.8590(7)°, *V* = 4069.14(17)

Å³, *Z* = 1, *T* = 123 (2) K, ρ_c = 1.535 g cm⁻³, μ (Mo-K α) = 0.514 cm⁻¹, $2\theta_{\max}$ = 50.0°, λ (Mo-K α) = 0.71074 Å, 40282 reflections measured, 18258 unique (*R*_{int} = 0.0223), 13311 (*I* > 2 σ (*I*)) were used to refine 1081 parameters, 0 restraints, *wR*₂ = 0.1875 (*I* > 2 σ (*I*)), *R*₁ = 0.0554 (*I* > 2 σ (*I*)), GOF = 1.111.

Crystal data for Rh₂(ppeb)₄(1-adamantylamine)₂ (1-AD**):** C₉₂H₇₀F₂₀N₂O₈Rh₂, *M_r* = 1965.32, triclinic, space group *P*-1, (#2), *a* = 10.8625(8), *b* = 13.8827(10), *c* = 14.9217(11) Å, α = 103.6458(15)°, β = 93.1519(15)°, γ = 94.0312(16)°, *V* = 2175.3(3) Å³, *Z* = 1, *T* = 123 (2) K, ρ_c = 1.500 g cm⁻³, μ (Mo-K α) = 0.483 cm⁻¹, $2\theta_{\max}$ = 50.0°, λ (Mo-K α) = 0.71074 Å, 21333 reflections measured, 9889 unique (*R*_{int} = 0.071), 8336 (*I* > 2 σ (*I*)) were used to refine 602 parameters, 6 restraints, *wR*₂ = 0.1511 (*I* > 2 σ (*I*)), *R*₁ = 0.0511 (*I* > 2 σ (*I*)), GOF = 1.089.

Results and discussion

Synthesis and Characterization

Synthesis of the Rh(II) complex was performed by the reaction of Na₄[Rh₂(CO₃)₄]·3H₂O with 8 eq. of Hppeb at 100 °C in dimethylacetamide/H₂O (3:1) for 8 h. A four substituted complex, Rh₂(ppeb)₄(Et₂O)₂, was obtained in 27% yield by subsequent column chromatography using neutral alumina (Et₂O as the eluent). Note that the use of Na₄[Rh₂(CO₃)₄]·3H₂O was crucial, and the reaction of Hppeb with carboxylate precursors, Rh(II) acetate or Rh(II) trifluoroacetate, did not afford the desired complex possibly due to the slow reaction rate of the di-substituted carboxylate complex.¹⁵ The slow evaporation of the THF/Et₂O mixed solution of Rh₂(ppeb)₄(Et₂O)₂ afforded single crystals of Rh₂(ppeb)₄(THF)₂

(**1-THF**) suitable for X-ray crystallography. **1-PN** and **1-AD** were also obtained by recrystallization of $\text{Rh}_2(\text{ppeb})_4(\text{Et}_2\text{O})_2$. The recrystallisation of $\text{Rh}_2(\text{ppeb})_4(\text{Et}_2\text{O})_2$ from slow evaporation of the mixed solution of $\text{Et}_2\text{O}/3$ -pentanone afforded $\text{Rh}_2(\text{ppeb})_4(3\text{-pentanone})_2$ (**1-PN**). To obtain $\text{Rh}_2(\text{ppeb})_4(1\text{-adamantylamine})_2$ (**1-AD**), recrystallisation was performed by layering Et_2O solution of 1-adamantylamine on Et_2O solution of $\text{Rh}_2(\text{ppeb})_4(\text{Et}_2\text{O})_2$. These three compounds were characterised by single-crystal X-ray diffraction and IR spectroscopy.

Crystal Structures

The crystal structure of **1-THF** is comprised of a Rh(II) paddle-wheel with THF molecules coordinated at the axial sites (Fig. 1a). Four ppeb ligands occupied the positions in the equatorial plane of each rhodium atom. The Rh1-Rh1' distance was 2.3875(13) Å, which is in the range found for previously

reported Rh(II) paddle-wheel dimers (2.316 to 2.486 Å).¹⁸ The angle between the phenylene and perfluorophenyl rings was estimated to be 18.4°.

In the crystal packing structure of **1-THF**, aforementioned multipoint Ar-Ar^F interaction played a key role in stabilising the molecular assembly. As shown in Fig. 1b, an infinite two-dimensional (2-D) square-grid sheet structure was formed via multipoint Ar-Ar^F interactions between the ligands. The mean interplanar separation between the phenylene and perfluorophenyl rings was 3.56(16) Å. These 2-D sheets were stacked through π - π interactions (denoted as blue line in Fig. 1b) to form a columnar structure of paddle-wheel units along the *c* axis. As a result, a porous structure with the channel entrance size¹⁹ of 13.8 x 12.1 Å² was formed (Fig. 1c), and THF molecules were contained in the pores as guests. The recrystallisation of $\text{Rh}_2(\text{ppeb})_4(\text{Et}_2\text{O})_2$ from $\text{Et}_2\text{O}/3$ -pentanone afforded a similar crystal structure composed of a Rh(II)

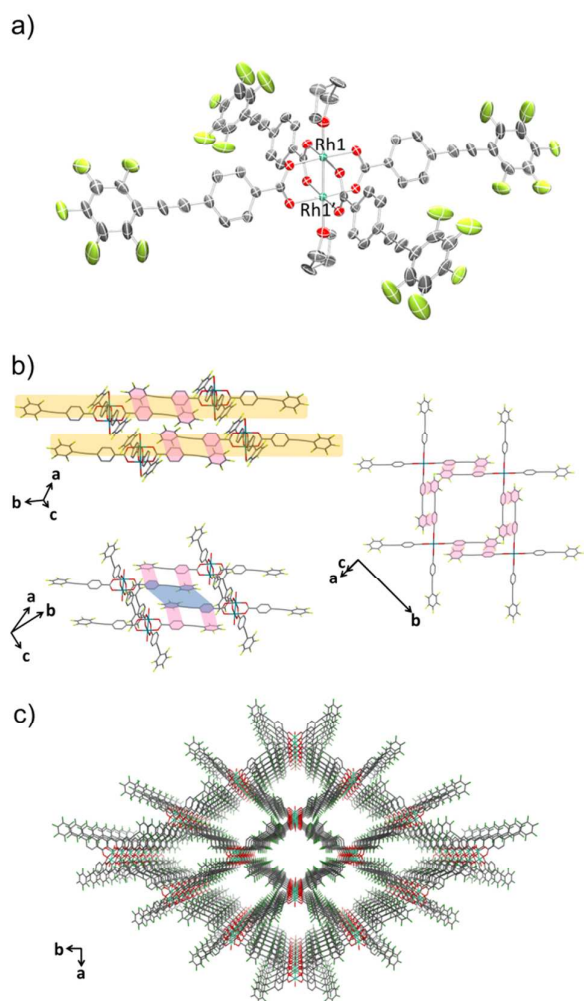


Fig. 1 (a) An ORTEP drawing of **1-THF** (50% probability ellipsoids). Hydrogen atoms are omitted for clarity. (b) 2-D sheet structure of **1-THF**. Ar-Ar^F interactions and π - π interactions are shown in red and blue lines respectively. Hydrogen atoms, carbon atoms of THF at the axial positions are omitted for clarity. (c) Crystal packing of **1-THF** along the *c* axis. Hydrogen atoms, carbon atoms of THF at the axial positions are omitted for clarity. O = red, C = grey, F = pale green, Rh = sea green.

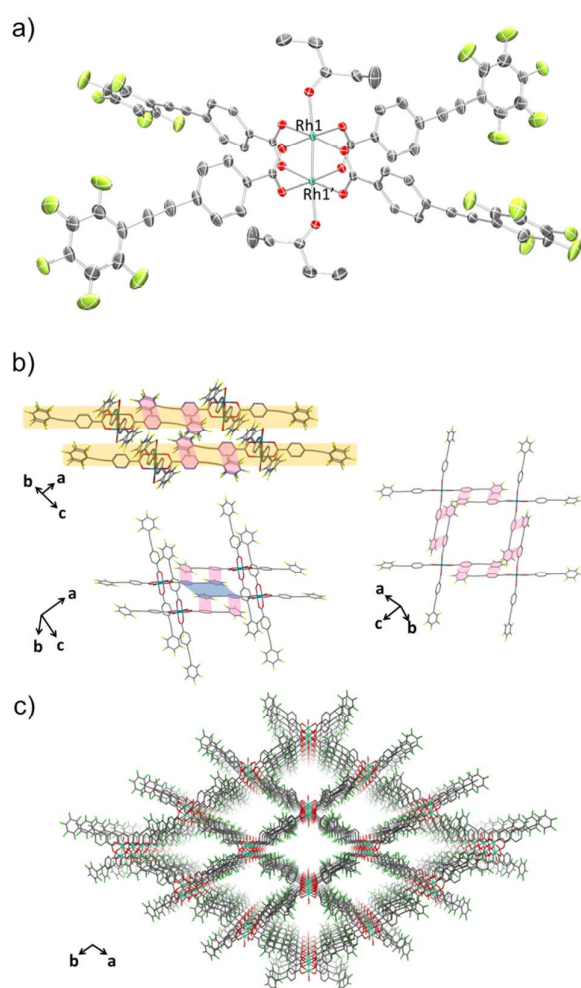


Fig. 2 (a) An ORTEP drawing of **1-PN** (50% probability ellipsoids). Hydrogen atoms and crystal solvent molecules are omitted for clarity. (b) 2-D sheet structure of **1-PN**. Ar-Ar^F interactions and π - π interactions are shown in red and blue lines respectively. Hydrogen atoms, carbon atoms of 3-pentanone at the axial positions and crystal solvent molecules observed in the channels are omitted for clarity. (c) Crystal packing of **1-PN** along the *c* axis. Hydrogen atoms, carbon atoms of 3-pentanone at the axial positions and crystal solvent molecules observed in the channels are omitted for clarity. O = red, C = grey, F = pale green, Rh = sea green.

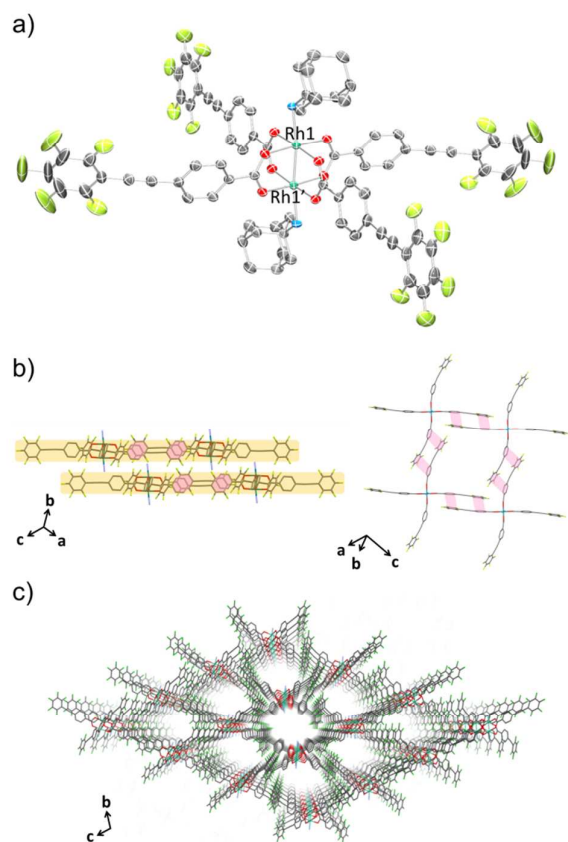


Fig. 3 (a) An ORTEP drawing of **1-AD** (50% probability ellipsoids). Hydrogen atoms and crystal solvent molecules are omitted for clarity. (b) 2-D sheet structure of **1-AD**. Ar-Ar^F interactions are shown in red lines. Hydrogen atoms, carbon atoms of 1-adamantylamine at the axial positions and crystal solvent molecules observed in the channels are omitted for clarity. (c) Crystal packing of **1-AD** along the *a* axis. Hydrogen atoms, carbon atoms of 1-adamantylamine at the axial positions and crystal solvent molecules observed in the channels are omitted for clarity. O = red, C = grey, F = pale green, Rh = sea green.

paddle-wheel complex bearing 3-pentanone at the axial sites, Rh₂(ppeb)₄(3-pentanone)₂ (**1-PN**) (Fig. 2). In the crystal structure of **1-PN**, the mean interplanar separation between phenylene and perfluorophenyl rings was 3.49(12) Å, and the channel entrance size was estimated to be 12.9 × 10.5 Å². It should be noted that the active sites of these complexes were exposed to the pores in both structures.

The reaction of Rh₂(ppeb)₄(Et₂O)₂ with 1-adamantylamine was subsequently performed to examine the adjustability of the framework to bulky molecules, and the targeted axial ligand substituted complex, Rh₂(ppeb)₄(1-adamantylamine)₂ (**1-AD**, Fig. 3a), was obtained. The distance between two rhodium atoms in **1-AD** was 2.4140(7) Å, which is comparable to that of **1-THF** or **1-PN**. For **1-AD**, the angles between the phenylene and perfluorophenyl rings were 16.3° and 5.9°. In the crystal structure of **1-AD**, a 2-D sheet structure stabilised by multipoint Ar-Ar^F interactions was also obtained (Fig. 3b). However, π-π interactions between the 2-D sheets were not observed because the bulkiness of the axial ligands prevented close contact between sheets. Alternatively, the ppeb⁻ ligands exhibited a conformation almost perpendicular to the 2-D

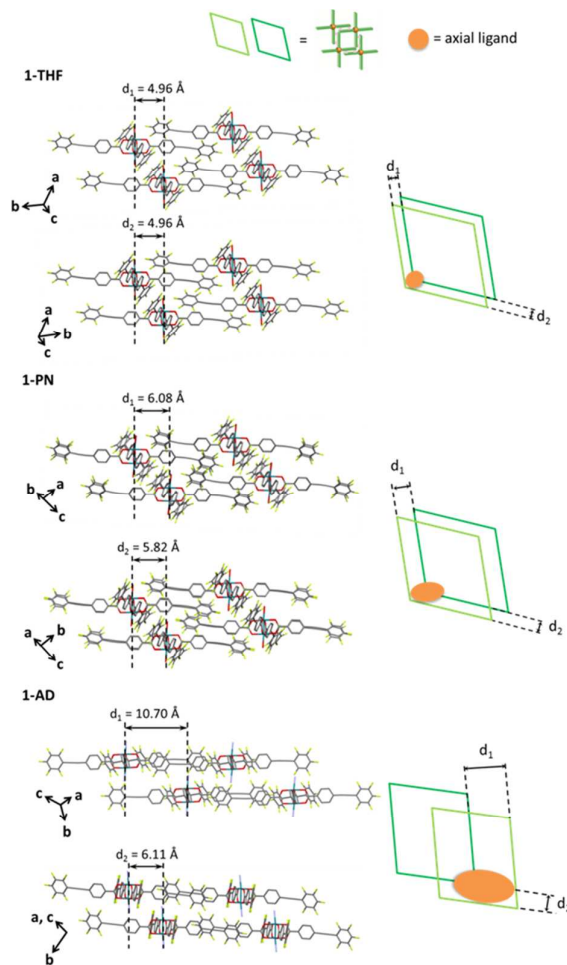


Fig. 4 Side view of the crystal packing (left) and the schematic illustration of the top view of the interlayer stacking structure (right) for **1-THF** (top), **1-PN** (middle) and **1-AD** (bottom). In the schematic illustration, the axial ligands are represented as orange circles.

sheets, and CF-π interactions²⁰ between the ppeb⁻ ligands formed inter-sheet stacking. As a result, a 1-D channel structure with an entrance size of 10.1 × 8.2 Å² was obtained (Fig. 3c). The mean interplanar separation between the phenylene and perfluorophenyl rings was 3.50(16) Å. The axial ligands were also exposed to the pores despite the different stacking mode from **1-THF** and **1-PN**. The comparison between the assembling-patterns between these structures is shown in Fig. 4. The horizontal distances between the Rh dimeric nodes in neighbouring 2-D sheets (denoted as *d*₁ and *d*₂) were found to be *d*₁ = *d*₂ = 4.96 Å for **1-THF**, *d*₁ = 6.08 Å, *d*₂ = 5.82 Å for **1-PN** and *d*₁ = 10.70 Å, *d*₂ = 6.11 Å for **1-AD** and were mainly different between the three structures, reflecting the bulkiness of the axial ligands. These crystallographic observations indicate that the 2-D sheet structures in these porous frameworks are well defined by the multipoint Ar-Ar^F interactions and that the interlayer stacking structures are controllable in response to the size and shape of the axial ligands.

The Effect of the Axial Ligands on the Porous Properties

The effect of the axial ligands on the porous properties of the frameworks was also investigated by several measurements. A TG curve of **1-AD** exhibited no weight loss upon heating up to 284 °C (Fig. 5c), which indicated the strong coordination ability of the axial ligands to the metal centres. Upon further heating up to 600 °C, the degradation of the complex was observed. It should be noted that the removal of the guest molecules (Et₂O) was not observed due to their highly volatile nature. The removal of the axial ligand was also not observed due to their strong coordination ability. Furthermore, the CO₂ adsorption isotherms for **1-AD** evacuated at 40 °C (Fig. 5f) and 120 °C (Fig. S1c in the ESI) exhibited almost identical sorption profiles, suggesting the retention of the porous structure due to the “capping” of active sites with strongly coordinated axial ligands. In contrast, the TG curves of **1-THF** and **1-PN** indicated the release of axial ligands in the temperature range of 100–170 °C with a weight loss of 5.30% (**1-THF**) and 5.82% (**1-PN**), respectively (Fig. 5a-b). The degradation of the complexes was observed in the temperature range of 327–600 °C. In the CO₂ adsorption isotherms of **1-THF** and **1-PN** evacuated at 40 °C and 120 °C, the amount of adsorbed CO₂ gradually increased as the pressure increased and showed hysteresis during the desorption process (Fig. 5d-e and Fig. S1a-b in the ESI) and the adsorption amount are dependent to the temperature of pre-treatment, which may be attributed to the transformation of the interlayer stacking structure arising from the exchange or the loss of the axial ligands. These results clearly indicate the difference in the lability of the axial ligands between **1-AD** and other two structures, **1-THF** and **1-PN**. Additionally, N₂ adsorption measurements at 77 and 195 K were performed and almost no adsorption of N₂ was observed for **1-THF** and **1-PN** (Fig. S2a-b and Fig. S3a-b in the ESI), suggesting the selective CO₂ adsorption over N₂ in these frameworks. In contrast to **1-THF** and **1-PN**, N₂ was slightly adsorbed to **1-AD** at 77 K (Fig. S2c in the ESI), although no adsorption of N₂ was observed at 195 K (Fig. S3c in the ESI).

PXRD measurements of the samples after the removal of guest and the dissociation of the axial ligands were performed to investigate the structural change in these processes. The experiments were performed for **1-AD** and **1-PN**, which have the unremovable axial ligands and the removable ligands, respectively. Note that the PXRD patterns for as-synthesized compounds were measured under the vapour of guest molecules to prevent the loss of guest molecules. In the case of **1-AD**, PXRD pattern changed after the evacuation at 40 °C (from A to B in Fig. S4 in the ESI), suggesting the structural change attributed to the removal of guest molecules. Subsequent evacuation of the sample at 120 °C gave the almost identical PXRD pattern (Fig. S4 C in the ESI), which indicates the strong coordination of axial ligands. These results are fully consistent with the result of TGA and CO₂ adsorption measurements. In the case of **1-PN**, PXRD pattern changed after evacuation at 40 °C (from D to E in Fig. S5 in the ESI) and the structural transformation accompanied by the removal of guest was observed. In contrast to **1-AD**, the subsequent

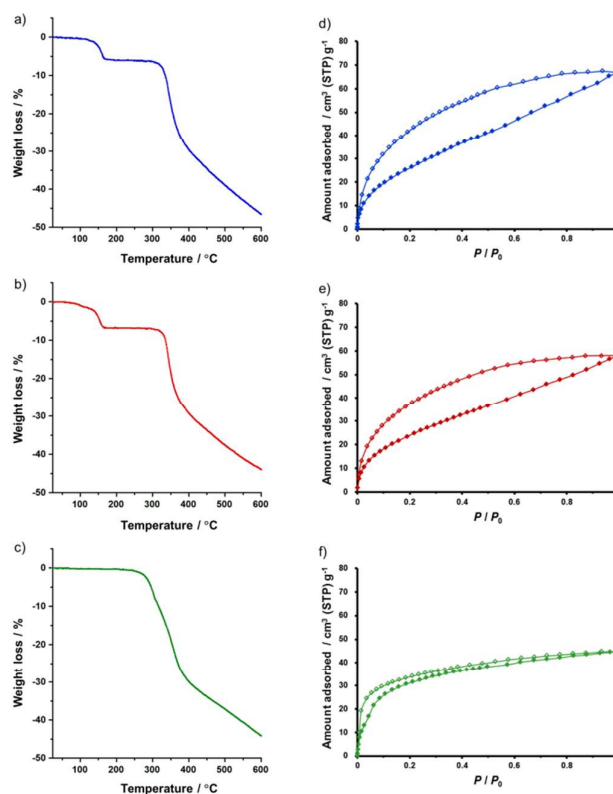


Fig. 5 TGA profiles of (a) **1-THF**, (b) **1-PN** and (c) **1-AD** with a heating rate of 20 K min⁻¹. CO₂ sorption isotherms of (d) **1-THF**, (e) **1-PN** and (f) **1-AD** at 195 K. Filled shapes: adsorption. Open shapes: desorption. The samples of **1-THF**, **1-PN** and **1-AD** for the CO₂ adsorption were evacuated at 40 °C before the measurements.

evacuation at 120 °C caused the significant change of the PXRD pattern (from E to F in Fig. S5 in the ESI) and the structural transformation due to the dissociation of the axial ligands was indicated. At this stage, we could not determine the structure after the removal of the guest molecules or the axial ligands, and thus, the detailed discussion on the CO₂ adsorption profiles was not allowed. However, the results of CO₂ adsorption and PXRD measurements revealed that the crystallinity and porosity of the sample were maintained throughout the removal of guest molecules and the dissociation of the axial ligands, and the framework structures transformed flexibly accompanied by these processes. Additionally, PXRD patterns before and after the CO₂ adsorption were also examined. As shown in Fig. S6-9, in the ESI, the samples of **1-PN** and **1-AD** did not show significant change in PXRD pattern after the CO₂ adsorption measurements regardless of the pre-treatment temperature. These results indicate that our frameworks recover their initial structures after the CO₂ adsorption/desorption processes.

Flexible Structural Transformation during the Ligand Exchange Reaction of the Frameworks

The structural flexibility of **1-THF** and **1-PN** and the reactivity of the open axial sites in these frameworks were examined by PXRD measurements. Initially, crystalline sample of **1-THF** was

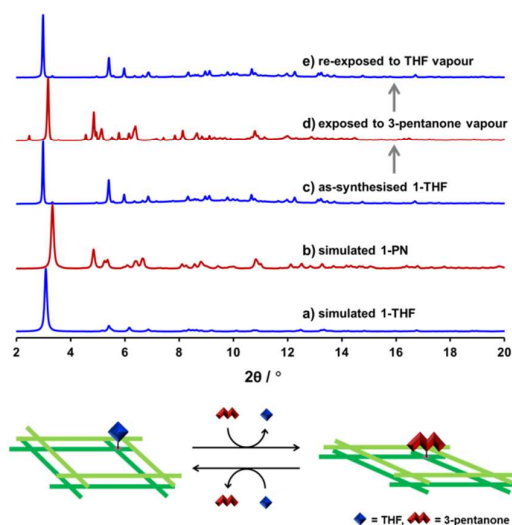


Fig. 6 Simulated XRD patterns of (a) **1-THF** and (b) **1-PN** and PXRD patterns of as-synthesised (c) **1-THF**, (d) the sample of **1-THF** exposed to 3-pentanone vapour, and (e) the sample re-exposed to THF vapour. Schematic illustration of the structural transformation between **1-THF** and **1-PN** induced by the reversible ligand substitution reaction (bottom). ($\lambda = 0.79978 \text{ \AA}$)

evacuated at room temperature for 1 h and exposed to 3-pentanone vapour for 1 h. PXRD patterns of before and after the treatment suggested the complete structural transformation from **1-THF** to **1-PN** (Fig. 6c-d, blue and red lines). Subsequently, obtained powder sample of **1-PN** was evacuated at room temperature for 1 h and exposed to THF vapour for 1 h. PXRD pattern of the sample treated with THF revealed the regeneration of **1-THF** (Fig. 6e). These results indicated that the active sites of the SBUs in our framework effectively worked to control the structural flexibility of each phase.

Conclusions

In conclusion, we demonstrated the construction and structural determination of porous frameworks composed of a substitution-inert complex with active sites. Three novel Rh(II) paddle-wheel complexes, $\text{Rh}_2(\text{ppeb})_4(\text{X})_2$ ($\text{X} = \text{THF}$ (**1-THF**), 3-pentanone (**1-PN**), and 1-adamantylamine (**1-AD**)), were successfully assembled to form porous frameworks with a solvent accessible columnar channel by utilizing multipoint Ar- Ar^{F} interaction. The obtained supramolecular structures possessed active sites exposed to the channel, and the comparison of crystal packing of the three complexes revealed the structural difference induced by the size and the structure of the axial ligands. Furthermore, the porous properties of these frameworks were also examined by several experiments. Although the axial ligands of **1-AD** did not dissociate upon heating and during the sorption process, the axial ligands of **1-THF** and **1-PN** were labile to the axial ligand substitution reaction, and the induced-fit structural transformation in response to the ligand substitution was observed in the crystalline state. We believe that our results presented here should be a key example to construct porous materials based

on substitution-inert metal ions with active sites that can be applied for catalytic reactions and chemical sensors.

Acknowledgements

This work was supported by a Grant-in-Aid for Young Scientists (A) (No. 15H05480) (to M.K.), a Grant-in-Aid for Young Scientists (A) (No. 25708011) (to S.M.), a Grant-in-Aid for Challenging Exploratory Research (No. 26620160) (to S.M.), and a Grant-in-Aid for JSPS Fellows (No. K252605890) (to T.I.) from the Japan Society for the Promotion of Science. This work was also supported by a Grant-in-Aid for Scientific Research on Innovative Areas "AnApple" (No. 15H00889). The synchrotron radiation experiments were performed at the BL02B2 of SPring-8 with the approval of the Japan Synchrotron Radiation Research Institute (JASRI) (Proposal No. 2014B1428).

Notes and references

- (a) B. Moulton, M. J. Zaworotko, *Chem. Rev.*, 2001, **101**, 1629-1658; (b) S. Kitagawa, R. Kitaura, S. Noro, *Angew. Chem. Int. Ed.*, 2004, **43**, 2334-2375; (c) G. Férey, C. Serre, *Chem. Soc. Rev.*, 2009, **38**, 1380-1399; (d) J. Lee, O. K. Farha, J. Roberts, K. A. Scheidt, S. T. Nguyen, J. T. Hupp, *Chem. Soc. Rev.*, 2009, **38**, 1450-1459; (e) M. D. Allendorf, C. A. Bauer, R. K. Bhakta, R. J. T. Houk, *Chem. Soc. Rev.*, 2009, **38**, 1330-1352; (f) D. Zacher, O. Shekhah, C. Wöll, R. A. Fischer, *Chem. Soc. Rev.*, 2009, **38**, 1418-1429; (g) K. Sumida, D. L. Rogow, J. A. Mason, T. M. McDonald, E. D. Bloch, Z. R. Herm, T.-H. Bae, J. R. Long, *Chem. Rev.*, 2012, **112**, 724-781; (h) M. Yoon, R. Srirambalaji, K. Kim, *Chem. Rev.*, 2012, **112**, 1196-1231; (i) J.-R. Li, J. Sculley, H.-C. Zhou, *Chem. Rev.*, 2012, **112**, 869-932; (j) C. Wang, T. Zhang, W. Lin, *Chem. Rev.*, 2012, **112**, 1084-1104; (k) H. Furukawa, K. E. Cordova, M. O'Keeffe, O. M. Yaghi, *Science*, 2013, **341**, 974-986.
- (a) Y. Inokuma, S. Yoshioka, J. Ariyoshi, T. Arai, Y. Hitora, K. Takada, S. Matsunaga, K. Rissanen, M. Fujita, *Nature*, 2013, **495**, 461-466; (b) B. D. Chandler, G. D. Enright, K. A. Udachin, S. Pawsey, J. A. Ripmeester, D. T. Cramb, G. K. H. Shimizu, *Nat. Mater.*, 2008, **7**, 229-235; (c) W. M. Bloch, A. Burgun, C. J. Coghlan, R. Lee, M. L. Coote, C. J. Doonan, C. J. Sumby, *Nat. Chem.*, 2014, **6**, 906-912; (d) J. Rabone, Y.-F. Yue, S. Y. Chong, K. C. Stylianou, J. Bacsá, D. Bradshaw, G. R. Darling, N. G. Berry, Y. Z. Khimiyak, A. Y. Ganin, P. Wiper, J. B. Claridge, M. J. Rosseinsky, *Science*, 2010, **329**, 1053-1057; (e) G. K. H. Shimizu, J. M. Taylor, S. Kim, *Science*, 2013, **341**, 354-355; (f) H. Deng, S. Grunder, K. E. Cordova, C. Valente, H. Furukawa, M. Hmadeh, F. Gándara, A. C. Whalley, Z. Liu, S. Asahina, H. Kazumori, M. O'Keeffe, O. Terasaki, J. F. Stoddart, O. M. Yaghi, *Science*, 2012, **336**, 1018-1023.
- (a) E. D. Bloch, W. L. Queen, R. Krishna, J. M. Zadrozny, C. M. Brown, J. R. Long, *Science*, 2012, **335**, 1606-1610; (b) S. Xiang, Z. Zhang, C. Zhao, K. Hong, X. Zhao, D. Ding, M. Xie, C. Wu, M. C. Das, R. Gill, K. M. Thomas, B. Chen, *Nat. Commun.* 2011, **2**, 204; (c) E. D. Bloch, M. R. Hudson, J. A. Mason, S. Chavan, V. Crocellà, J. D. Howe, K. Lee, A. L. Dzubak, W. L. Queen, J. M. Zadrozny, S. J. Geier, L.-C. Lin, L. Gagliardi, B. Smit, J. B. Neaton, S. Bordiga, C. M. Brown, J. R. Long, *J. Am. Chem. Soc.*, 2014, **136**, 10752-10761; (d) Y.-S. Bae, C. Y. Lee, K. C. Kim, O. K. Farha, P. Nickias, J. T. Hupp, S. T. Nguyen, R. Q. Snurr, *Angew. Chem. Int. Ed.*, 2012, **51**, 1857-1860; (e) Z. Guo, H. Wu, G. Srinivas, Y. Zhou, S. Xiang, Z. Chen, Y. Yang,

- W. Zhou, M. O'Keeffe, B. Chen, *Angew. Chem. Int. Ed.*, 2011, **50**, 3178-3181.
- 4 (a) C.-D. Wu, A. Hu, L. Zhang, W. Lin, *J. Am. Chem. Soc.*, 2005, **127**, 8940-8941; (b) Z. Zhang, Y. Chen, S. He, J. Zhang, X. Xu, Y. Yang, F. Nosheen, F. Saleem, W. He, X. Wang, *Angew. Chem. Int. Ed.*, 2014, **53**, 12517-12521; (c) W. Xuan, C. Ye, M. Zhang, Z. Chen, Y. Cui, *Chem. Sci.*, 2013, **4**, 3154-3159.
- 5 (a) B. Chen, Y. Yang, F. Zapata, G. Lin, G. Qian, E. B. Lobkovsky, *Adv. Mater.*, 2007, **19**, 1693-1696; (b) N. B. Shustova, A. F. Cozzolino, S. Reineke, M. Baldo, M. Dincă, *J. Am. Chem. Soc.*, 2013, **133**, 13326-13329.
- 6 (a) S. S.-Y. Chui, S. M.-F. Lo, J. P. H. Charmant, A. G. Orpen, I. D. Williams, *Science* 1999, **283**, 1148-1150; (b) N. L. Rosi, J. Kim, M. Eddaoudi, B. Chen, M. O'Keeffe, O. M. Yaghi, *J. Am. Chem. Soc.*, 2005, **127**, 1504-1518.
- 7 (a) P. Ceccherelli, M. Curini, M. C. Marcotullio, O. Rosati, *Tetrahedron*, 1991, **47**, 7403-7408; (b) M. P. Doyle, *Acc. Chem. Res.*, 1986, **19**, 348-356; (c) M. P. Doyle, K. G. High, C. L. Neslonely, T. W. Clayton Jr., J. Lin, *Organometallics*, 1991, **10**, 1225-1226; (d) S. Tanaka, S. Masaoka, K. Yamauchi, M. Annaka, K. Sakai, *Dalton Trans.*, 2010, **39**, 11218-11226; (e) D. K. Kumar, A. S. Filatov, M. Napier, J. Sun, E. V. Dikarev, M. A. Petrukhnina, *Inorg. Chem.*, 2012, **51**, 4855-4861; (f) J. Hansen, H. M. L. Davies, *Coord. Chem. Rev.*, 2008, **252**, 545-555; (g) K. P. Kornecki, J. F. Briones, V. Boyarskikh, F. Fullilove, J. Autschbach, K. E. Schrote, K. M. Lancaster, H. M. L. Davies, J. F. Berry, *Science*, 2013, **342**, 351-354.
- 8 (a) G. Férey, C. Serre, C. Mellot-Draznieks, F. Millange, S. Surblé, J. Dutour, I. Margiolaki, *Angew. Chem. Int. Ed.*, 2004, **43**, 6296-6301; (b) G. Férey, C. Mellot-Draznieks, C. Serre, F. Millange, S. Surblé, J. Dutour, I. Margiolaki, *Science*, 2005, **309**, 2040-2042.
- 9 (a) P. D. C. Dietzel, Y. Morita, R. Blom and H. Fjellvåg, *Angew. Chem. Int. Ed.*, 2005, **44**, 6354-6358; (b) B. Chen, N. W. Ockwig, A. R. Millward, D. S. Contreras and O. M. Yaghi, *Angew. Chem. Int. Ed.*, 2005, **44**, 4745-4749; (c) X.-S. Wang, S. Ma, P. M. Forster, D. Yuan, J. Eckert, J. J. López, B. J. Murphy, J. B. Parise and H.-C. Zhou, *Angew. Chem. Int. Ed.*, 2008, **47**, 7263-7266; (d) D. Yuan, D. Zhao, D. Sun, and H.-C. Zhou, *Angew. Chem. Int. Ed.*, 2010, **49**, 5357-5361; (e) M. Dincă, A. Dailly, Y. Liu, C. M. Brown, D. A. Neumann and J. R. Long, *J. Am. Chem. Soc.*, 2006, **128**, 16876-16883; (f) T. M. McDonald, D. M. D'Alessandro, R. Krishnac and J. R. Long, *Chem. Sci.*, 2011, **2**, 2022-2028; (g) Y. Liu, J. F. Eubank, A. J. Cairns, J. Eckert, V. C. Kravtsov, R. Luebke and M. Eddaoudi, *Angew. Chem. Int. Ed.*, 2007, **46**, 3278-3283; (h) M. Pang, A. J. Cairns, Y. Liu, Y. Belmabkhout, H. C. Zeng and Mohamed Eddaoudi, *J. Am. Chem. Soc.*, 2012, **134**, 13176-13179.
- 10 (a) P. Li, Y. He, J. Guang, L. Weng, J. C.-G. Zhao, S. Xiang and B. Chen, *J. Am. Chem. Soc.*, 2014, **136**, 547-549; (b) W. Yang, A. Greenaway, X. Lin, R. Matsuda, A. J. Blake, C. Wilson, W. Lewis, P. Hubberstey, S. Kitagawa, N. R. Champness and M. Schröder, *J. Am. Chem. Soc.*, 2010, **132**, 14457-14469; (c) M. Mastalerz and I. M. Opper, *Angew. Chem. Int. Ed.*, 2012, **51**, 5252-5255; (d) S. A. Dalrymple and G. K. H. Shimizu, *J. Am. Chem. Soc.*, 2007, **129**, 12114-12116; (e) P. S. Nugent, V. Lou Rhodus, T. Pham, K. Forrest, L. Wojtas, B. Space and Michael J. Zaworotko, *J. Am. Chem. Soc.*, 2013, **135**, 10950-10953; (f) P. Li, Y. He, Y. Zhao, L. Weng, H. Wang, R. Krishna, H. Wu, W. Zhou, M. O'Keeffe, Y. Han and B. Chen, *J. Am. Chem. Soc.*, 2015, **54**, 574-577.
- 11 (a) M. J. Bojdys, M. E. Briggs, J. T. A. Jones, D. J. Adams, S. Y. Chong, M. Schmidtman and A. I. Cooper, *J. Am. Chem. Soc.*, 2013, **135**, 16566-16571; (b) T. Kaczorowski, I. Justyniak, T. Lipińska, J. Lipkowski and J. Lewiński, *J. Am. Chem. Soc.*, 2009, **131**, 5393-5395; (c) M. Mastalerz, M. W. Schneider, I. M. Opper and O. Presly, *Angew. Chem. Int. Ed.*, 2011, **50**, 1046-1051; (d) K. Sokolowski, W. Bury, I. Justyniak, D. Fairén-Jimenez, K. Soltys, D. Prochowicz, S. Yang, M. Schröder and Janusz Lewiński, *Angew. Chem. Int. Ed.*, 2013, **52**, 13414-13418; (e) G. Zhang, O. Presly, F. White, I. M. Opper and M. Mastalerz, *Angew. Chem. Int. Ed.*, 2014, **53**, 1516-1520; (f) C. Redshaw, S. Jana, C. Shang, M. R. J. Elsegood, X. Lu and Z. X. Guo, *Organometallics*, 2010, **29**, 6129-6132.
- 12 (a) J. Lü, C. Perez-Krap, M. Suyetin, N. H. Alsmail, Y. Yan, S. Yang, W. Lewis, E. Bichoutskaia, C. C. Tang, A. J. Blake, R. Cao and M. Schröder, *J. Am. Chem. Soc.*, 2014, **136**, 12828-12831; (b) W. Bury, I. Justyniak, D. Prochowicz, A. Rola-Noworyta and Janusz Lewiński, *Inorg. Chem.*, 2012, **51**, 7410-7414; (c) J. Lewiński, T. Kaczorowski, D. Prochowicz, T. Lipińska, I. Justyniak, Z. Kaszkur and J. Lipkowski, *Angew. Chem. Int. Ed.*, 2010, **49**, 7035-7039.
- 13 (a) H. Kim, Y. Kim, M. Yoon, S. Lim, S. M. Park, G. Seo and K. Kim, *J. Am. Chem. Soc.*, 2010, **132**, 12200-12202; (b) T. Tozawa, J. T. A. Jones, S. I. Swamy, S. Jiang, D. J. Adams, S. Shakespeare, R. Clowes, D. Bradshaw, T. Hasell, S. Y. Chong, C. Tang, S. Thompson, J. Parker, A. Trewin, J. Bacsa, A. M. Z. Slawin, A. Steiner and A. I. Cooper, *Nature Mat.*, 2009, **8**, 973-978; (c) J. T. A. Jones, T. Hasell, X. Wu, J. Bacsa, K. E. Jelfs, M. Schmidtman, S. Y. Chong, D. J. Adams, A. Trewin, F. Schiffman, F. Cora, B. Slater, A. Steiner, G. M. Day and A. I. Cooper, *Nature*, 2011, **474**, 367-361; (d) C. G. Bezzu, M. Helliwell, J. E. Warren, D. R. Allan, N. B. McKeown, *Science*, 2010, **327**, 1627-1630; (e) T. Hasell, S. Y. Chong, M. Schmidtman, D. J. Adams and A. I. Cooper, *Angew. Chem. Int. Ed.*, 2012, **51**, 7154-7157; (f) M. W. Schneider, I. M. Opper, A. Griffin and M. Mastalerz, *Angew. Chem. Int. Ed.*, 2013, **52**, 3611-3615.
- 14 (a) J. H. Williams, *Acc. Chem. Res.*, 1993, **26**, 593-598; (b) C. R. Patrick, G. S. Prosser, *Nature*, 1960, **187**, 1021.
- 15 T. Itoh, M. Kondo, M. Kanaïke, S. Masaoka, *CrystEngComm.*, 2013, **15**, 6122-6126.
- 16 C. R. Willson, H. Taube, *Inorg. Chem.*, 1975, **47**, 533-535.
- 17 G. M. Sheldrick, *Program for Crystal Structure Refinement, University of Göttingen, Germany*, 1997.
- 18 (a) F. A. Cotton, C. A. Murillo, R.A. Walton, "Multiple Bonds Between Metal Atoms", 3rd ed., Springer Science and Business Media, New York, 2005; (b) E. B. Royer, S. D. Robinson, *Platinum Metals Rev.*, 1982, **26**, 65-69.
- 19 The channel entrance size was estimated by considering the van der Waals radii of constituent atoms, and the atoms at axial ligands are omitted for the calculation.
- 20 (a) N. Hayashi, T. Mori, K. Matsumoto, *Chem. Commun.*, 1998, 1905-1906; (b) K. Reichenbacher, H. I. Süß, J. Hulliger, *Chem. Soc. Rev.*, 2005, **34**, 22-30; (c) X. Xu, B. Pooi, H. Hirao, S. H. Hong, *Angew. Chem. Int. Ed.*, 2014, **53**, 1283-1287.